Application of Sponge Boundary Conditions to Large-Eddy Simulation of Multiple Thermal Plumes

Chandra Shekhar Pant and Amitabh Bhattacharya

Abstract While numerically simulating multiple thermal plumes, instabilities arise at the inflow/outflow/convective (IOC) boundaries due to the inability of IOC boundary conditions to effectively advect the flow structures out of the computational domain. To address this issue, Large Eddy Simulation of multiple thermal plumes is carried out with a novel viscous sponge layer, recently formulated by Pant and Bhattacharya (Comput Fluids 134:177–189, 2016, [5]). We validate our results with available literature, and we also present the effect of sponge layer on vortex rings (produced by thermal bubbles) traveling at an oblique angle to the outflow boundary. It is concluded from this study that the sponge layer does not appreciably affect the vortex rings outside the layer. The vortex rings do get smoothened out inside the sponge layer, which ensures a smooth convective outflow velocity for the eddies, and leads to stable LES of thermal plumes.

1 Introduction

Pure multiple thermal plumes commonly exist in both natural and industrial processes. Interaction of multiple jets/plumes can be seen as a simplified model for interacting atmospheric clouds. In the context of deep clouds, Baines and Keffer [1] experimentally studied multiple jets of air at ambient temperature. Kaye and Linden [4] experimentally studied interaction of two axi-symmetric turbulent plumes and proposed a model. Recently, Cenedese and Linden [2] studied the dynamics of the two coalescing plumes and proposed a net (or "effective") entrainment constant for the multiple plumes. Numerical simulation of multiple plumes remain challenging because of the inadequacy of the proper boundary conditions. In this manuscript we performed Large Eddy Simulation (LES) of multiple plumes using the sponge boundary condition proposed by Pant and Bhattacharya [5]. To illustrate the effect of the viscous sponge layer on the flow structures, we also present results on isolated vortex rings impinging the sponge layer at an angle.

C.S. Pant · A. Bhattacharya (✉)
Indian Institute of Technology Bombay, Powai, Mumbai 400076, India
e-mail: bhattach@gmail.com

R. Örlü et al. (eds.), *Progress in Turbulence VII*, Springer Proceedings in Physics 196, DOI 10.1007/978-3-319-57934-4_34

2 Flow Domain, Governing Equations and Viscous Sponge Layer Formulation

A cuboidal computational domain is used, with dimension of $L_x \times L_y \times L_z$. Figure 1a shows the two dimensional schematic of the computational box. The complete non-dimensional equations for velocity field $\mathbf{u}$, pressure P and temperature, T used in this work are given as:

$$\nabla \cdot \mathbf{u} = 0 \tag{1}$$

$$\frac{\partial \mathbf{u}}{\partial t} + \mathbf{u} \cdot \nabla \mathbf{u} = -\nabla P + (\mathrm{Ri}) T \mathbf{j} - \nabla \cdot \sigma^t + \mathbf{b}^s \tag{2}$$

$$\frac{\partial T}{\partial t} + \mathbf{u} \cdot \nabla T = -\nabla \cdot \mathbf{Q} \tag{3}$$

Here, $\mathrm{Ri} = \beta \Delta T$ refers to the Richardson number, which is used to couple temperature and velocity evolution equations. $\mathbf{j}$ is the unit vector in the positive y direction, σ^t is the stress tensor due to unresolved turbulent scales and $\mathbf{Q}$ is the heat flux vector. Terms σ^t and $\mathbf{Q}$ are modeled using standard Smagorinsky-Lilly model [6]. $\mathbf{b}^s$ is the body force due to artificial viscosity in the sponge, given by:

$$b_i^s = H(\mathbf{x}) \nu^s \frac{1}{h_1 h_2 h_3} \left[\frac{\partial}{\partial \xi_1} \left(\frac{h_2 h_3}{h_1} \right) \frac{\partial v_i}{\partial \xi_1} + \frac{\partial}{\partial \xi_3} \left(\frac{h_1 h_2}{h_3} \right) \frac{\partial v_i}{\partial \xi_3} \right] \tag{4}$$

the term H(**x**) is 1 inside the sponge layer and 0 outside the domain, ν^s is the artificial viscosity. This novel sponge layer formulation allows a discontinuous jump in viscosity, so that the flow structures get dissipated inside the sponge layer. The detailed

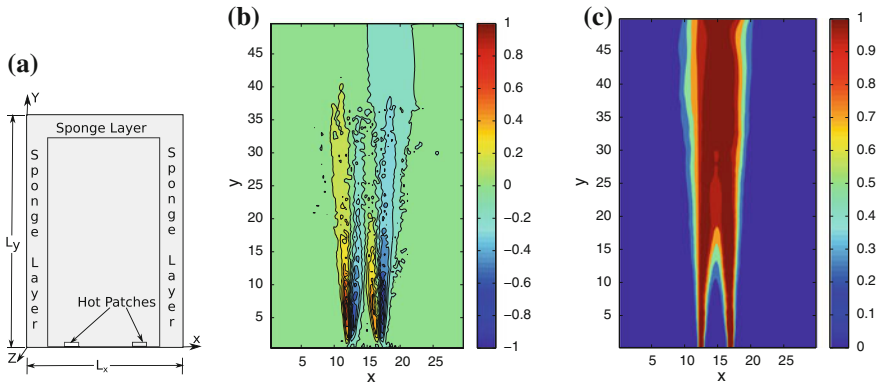

Fig. 1 **a** Schematic of computational domain. Time contour plots corresponding to case A1 of **b** average vorticity, $\langle \omega_3 \rangle$, and **c** average temperature field $\langle T \rangle(\mathbf{x})$ normalized with respect to temperature at $x = 2L_x/5$, $z = L_z/2$ ($x = 2L_x/5$, $z = L_z/2$ refers to the location of one of the hot patch at the bottom of computational domain)

formulation and solution procedure is explained in [5]. In this manuscript we assume that the flow has infinite Reynolds number, therefore Richardson number (Ri) is the only the free non-dimensional parameter.

3 Results

3.1 Simulation of Multiple Plumes

Two hot patches ($T = 1$) are introduced at the bottom of domain to simulate multiple thermal plumes, as shown in the Fig. 1a. No penetration boundary condition is used for the velocity field on the bottom plane ($y = 0$). The other boundary conditions are same as that explained in [5]. Two set of simulations (cases A1 and A2) are performed with different sponge layer viscosity ν_s. The parameters of the simulations are given in Table 1. In Fig. 2, the volume averaged kinetic energy is plotted against time for case A1 and A2, and it appears that both the simulations are stable for a long time. The contour plots of vorticity and normalized temperature field averaged in time are shown in Fig. 1b and c respectively. The intermixing between the two plumes and irrotationality of ambient velocity field is clearly evident from Fig. 1b. Figure 1c clearly shows that two thermal plumes develop independently until the axial distance of 10. Thereafter, the two thermal plumes start interacting with each other, and, beyond a certain height, become indistinguishable. These features of different flow regimes have been characterized by Cenedese and Linden [2].

Table 1 Simulation parameters for multiple thermal plume

Case	$L_x \times L_y \times L_z$	$N_x \times N_y \times N_z$	ν^s
A1	$30 \times 50 \times 30$	$113 \times 190 \times 113$	0.02
A2	$30 \times 50 \times 30$	$113 \times 190 \times 113$	0.05

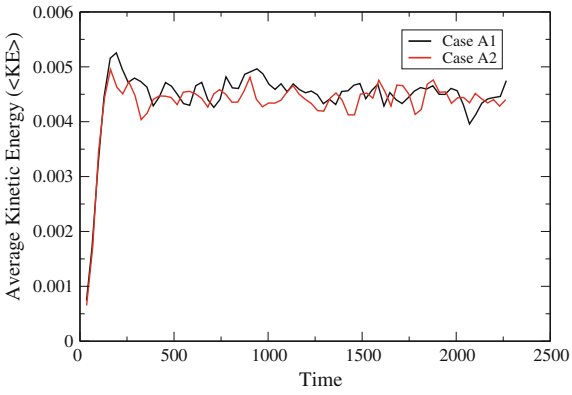

Fig. 2 Volume averaged kinetic energy $\frac{1}{2L_xL_yL_z}\int_{\mathscr{D}} u_i u_i d\mathbf{x}$ versus time for cases A1 and A2

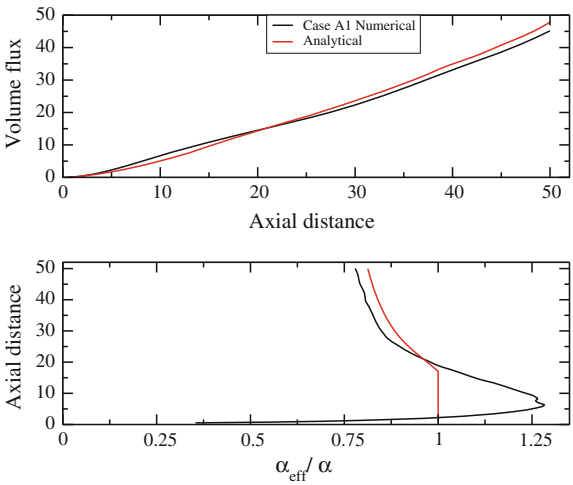

Fig. 3 Variation of volume flux and ratio of entrainment coefficient with axial distance

The total volume flux of two plumes (Q) and ratio of entrainment coefficients α_{eff}/α of the present LES simulations are validated against the analytical results of Cenedese and Linden [2] (shown in Fig. 3). Here F is the combined buoyancy flux for two plumes, α is the entrainment for single plume and α_{eff} is the net entrainment rate coefficient for the two interacting plumes. Unlike the analytical results, the ratio α_{eff}/α is significantly larger than 1 for $y < 20$ (y is the axial distance), which could be due to the relatively small value of y/D (D is the diameter of the patch). However, for $y > 20$, the agreement between simulation and analysis is reasonably good.

3.2 *Effect of the Sponge Layer on Flow Structures*

The LES of multiple thermal plumes is numerically stable, mainly due to the smoothening of flow structures near the convective outflow boundary. To illustrate the effect of the sponge layer on flow structures, we have carried out LES simulations of a thermal bubble, which then gives rise to a disintegrating vortex ring. The initial temperature field inside the bubble is spherically symmetric, with radius $r_c = 1.25$, centered at $(x_c, y_c, z_c) = (40, 1.25, 5)$. The initial temperature field is adapted from [3] and given by:

$$T = \begin{cases} 0, & r > r_c \\ A[1 + \cos(\pi \times r/r_c)], & r \leq r_c \end{cases}$$

where, $r = \sqrt{(x - x_c)^2 + (y - y_c)^2 + (z - z_c)^2}$ and $A = 0.5$.

Acceleration due to gravity has been tilted by 45 degrees to $-g(\mathbf{i} + \mathbf{j})/\sqrt{2}$ for these cases, so that the bubble impinges at an angle to the sponge layer. Velocity at

Table 2 Simulation parameters for vortex ring-sponge layer interactions

Case	$L_x \times L_y \times L_z$	$N_x \times N_y \times N_z$
B1	$80 \times 20 \times 10$	$400 \times 150 \times 100$
B2	$80 \times 40 \times 10$	$400 \times 300 \times 100$

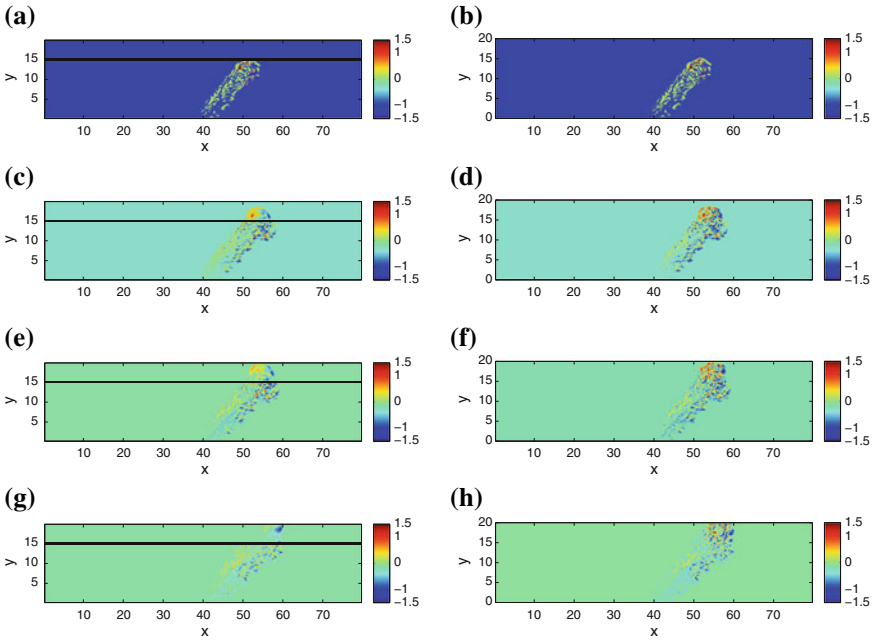

Fig. 4 Contour plot of vorticity ω_3 for case B1 at $z = L_z/2$: **a**, **c**, **e**, **g** and for case B2: **b**, **d**, **f**, **h**. Snapshots at the same row correspond to exactly the same time instant for both cases. A reference line has been drawn at $y = 15$, indicating the starting point of the top sponge layer in case B1

the bottom wall is set zero. Neumann boundary condition is used for top and lateral boundaries. The value of Ri is set 0.25. Table 2 lists the size of the computational box for the case B1 and case B2. The domain height L_y of case B1 is half that of case B2, and, correspondingly, the sponge layer height is 5, ranging from $y = 15$ to $y = 20$, which is again half compared to the case B2 (sponge height is 10, extends from $y = 20$ to $y = 30$). The domain in lateral and tangential directions is same for both cases. The grid resolution for both the cases is same. The iso-contours of vorticity at same time instants are compared for case B1 and case B2. These plots are shown before and after the penetration of vortex ring into the sponge layer $y = 15$ (Fig. 4). For case B1, outside the sponge layer (i.e. for $y < 15$) the flow structures look identically similar to case B2 (where, effectively, sponge layer is not present). At the same time, the sponge layer ensures that the flow structures are smooth near the convective outflow boundary, leading to stable simulations.

4 Conclusion

We have demonstrated that the novel viscous sponge layer scheme by [5] leads to stable LES for multiple plumes, allowing for long simulations over which statistics can be gathered. We found reasonable agreement of the net entrainment rate coefficient with analytical expressions by [2]. However, a taller computational domain may be needed to improve the agreement. The sponge layer formulation can be useful for LES of atmospheric flows, where multiple thermal plumes often interact with each other.

Acknowledgements AB acknowledges support from I.I.T. Bombay seed grant (Project Code 12IRCCSG020) for this work.

References

1. W.D. Baines, J.F. Keffer, Entrainment by a multiple source turbulent jet. Adv. Geophys. **18**, 289–298 (1975)
2. C. Cenedese, P. Linden, Entrainment in two coalescing axisymmetric turbulent plumes. J. Fluid Mech. **752**, R2 (2014)
3. F.X. Giraldo, M. Restelli, A study of spectral element and discontinuous Galerkin methods for the Navier–Stokes equations in nonhydrostatic mesoscale atmospheric modeling: equation sets and test cases. J. Comput. Phys. **227**(8), 3849–3877 (2008)
4. N. Kaye, P. Linden, Coalescing axisymmetric turbulent plumes. J. Fluid Mech. **502**, 41–63 (2004)
5. C.S. Pant, A. Bhattacharya, A viscous sponge layer formulation for robust large eddy simulation of thermal plumes. Comput. Fluids **134**, 177–189 (2016)
6. J. Smagorinsky, General circulation experiments with the primitive equations: I. The basic experiment. Mon. Weather Rev. **91**(3), 99–164 (1963)